



ELSEVIER

Available online at www.sciencedirect.com

SCIENCE @ DIRECT®

Nuclear Instruments and Methods in Physics Research B 207 (2003) 415–423

NIM B
Beam Interactions
with Materials & Atoms

www.elsevier.com/locate/nimb

Dynamic Monte Carlo simulation for reactive sputtering of aluminium

Z.Y. Chen ^{a,*}, A. Bogaerts ^a, D. Depla ^b, V. Ignatova ^a

^a Department of Chemistry, University of Antwerp (UIA), Universiteitsplein 1, B-2610 Wilrijk-Antwerp, Belgium

^b Department of Solid State Sciences, University of Gent, Krijgslaan 281 (S1), B-9000 Gent, Belgium

Received 10 December 2002; received in revised form 11 February 2003

Abstract

We have applied TRIDYN to simulate the transition from the metallic sputtering to the reactive sputtering mode during magnetron sputtering for an Al target when oxygen is added to argon plasma. Changes in the thickness and composition of multicomponent targets are investigated. The results basically confirm the reactive ion implantation mechanism together with chemical reaction in the subsurface. When oxygen mole fraction $x < 0.14$, the target surface never becomes fully oxidized, even for very long sputtering times. When $x > 0.14$ the target surface can be more or less fully oxidized. Furthermore, an abrupt change in the surface erosion rate at $x = 0.03$ is observed. This corresponds to the avalanche phenomenon indicating the sputtering mode transition.

© 2003 Elsevier Science B.V. All rights reserved.

PACS: 68.49.Sf; 79.20.Rf

Keywords: Reactive sputtering; Ion implantation; Magnetron discharge

1. Introduction

By adding a reactive gas to the conventional argon magnetron sputtering process, it is possible to deposit layers of oxides, nitrides, carbides and other compounds depending on the reactive gas used (e.g. [1–4]). It has been noticed that in reactive sputtering avalanche-like changes may occur in film deposition parameters such as deposition rate, discharge voltage, or plasma emission intensity, at a critical

flow rate of the reactive gas [5–9]. This avalanche-like change has been called a mode transition. Several models have been formulated to explain the observed changes of the target voltage and deposition rate as a function of reactive gas flow [5–9]. They described the dynamic balance between compound formation and the target surface and its dissociation by the sputtering process as a function of the deposition parameter, under the assumption that the compound formation is induced by chemisorption. However, no clear evidence for this mechanism has been given. It is interesting to notice that the above-mentioned models remain valid if one assumes another mechanism for surface modification than compound formation by

* Corresponding author. Tel.: +32-3-820-2383; fax: +32-3-820-2376.

E-mail address: chen@uia.ua.ac.be (Z.Y. Chen).

chemisorption, as long as the sputter yield is reduced and the secondary electron emission is changed by this target surface modification.

Recently, Depla and De Gryse (DG), performed some experiments on reactive sputtering of Si in a nitrogen/argon plasma [10] and of Al in an oxygen/argon plasma [4]. They showed the importance of ion implantation, also called subplantation, during reactive sputtering. In the latter experiment [4], a transition from metallic to poisoning mode takes place when a critical value of oxygen partial pressure equal to 0.23 is reached. The authors checked carefully the relationship between chemisorption and the changes in the target surface and found that chemisorption cannot account for the target surface modification and the sputtering mode transition. DG thus proposed the mechanism of reactive ion implantation to explain the sputtering mode transition and the target surface voltage changes during reactive sputtering. The mechanism is based on the subsurface compound formation by reaction between implanted reactive ions and the target atoms. During reactive sputtering ions become implanted in the target. Their concentration is inversely proportional to the erosion rate of the target. The target atoms react with the implanted ions to form a compound, which reduces the erosion rate of the target. This results in an increase of the implanted ion target concentration. Consequently, more target atoms react, further reducing the erosion rate. This avalanche finally results in an abrupt transition during the reactive magnetron process [4].

The aim of the present work is to examine the reactive ion implantation mechanism proposed in [4] by means of computer simulation. For this purpose, the dynamic Monte Carlo program TRIDYN [11,12] was applied, which is based on the static TRIM program (e.g. [13]) using the binary collision approximation (BCA) for ion beam–solid interaction. Other dynamic versions of the TRIM code, such as C-DYN [14] have similar main features and have also been applied to study Al oxidation under O bombardment or Ar ion bombardment in the presence of oxygen. TRIDYN (Version 4), in contrast to static versions, can simulate the dynamic change of surface position due to erosion or deposition and/or of the

composition of multicomponent targets during high-fluence ion implantation or ion-beam-assisted deposition. It allows for up to 5 different atomic species in the target and/or in the beam to be considered, with different energies and angles of incidence for the beam components. It is capable of predicting correctly the depth profiles of all atomic species in the target as a function of fluence of the incident projectiles. Additionally, sputtering yields, total areal densities, surface concentrations and re-emitted amounts are calculated as a function of fluence, as well as the surface erosion (when sputtering prevails) or thickness of deposited layer (when deposition prevails). TRIDYN is thus a very suitable tool to simulate the reactive sputtering of aluminium in an argon/oxygen plasma in a magnetron discharge.

Although considerable efforts have been made in modelling of magnetron discharges on the basis of fluid models [15,16], particle tracing [17,18], a hybrid model and the self-consistent particle model (e.g. [19,20] and references therein), here we will not consider how the magnetron discharge itself is modelled. Instead we will use experimental data for the target surface voltage and the sputtering time as the input parameters for the TRIDYN program. Moreover, the characteristics of the argon/oxygen plasma in the magnetron discharge employed in [4] are so complicated that we have to make some necessary but reasonable assumptions before applying TRIDYN to the reactive sputtering. In the next section the assumptions will be discussed in detail.

2. Model description

To simplify the simulation processes of the DG's reactive sputtering experiment using TRIDYN, several assumptions have been made. First of all, in the real experiment there are many kinds of positive ions and atoms/molecules which can impinge on the target surface (i.e. Ar^+ , O_2^+ , O^+ , Ar, O_2 and O). In our simulation, only two kinds of positive ions Ar^+ and O_2^+ are taken into account to reach the target surface, because they are dominant among the positive ions under DG's experimental condition. Secondly, the ratio of Ar^+ and

O_2^+ fluxes is assumed to be proportional to the ratio of partial pressures of Ar and O_2 . Thirdly, because in a magnetron discharge the incident energies of Ar^+ and O_2^+ ions bombarding the target surface are typically more than 80% of the discharge voltage [20], the positive ions bombarding the target surface are assumed to have a fixed energy of 360 eV in connection with DG's experiment (i.e. typical discharge voltage of 375 V), although in reality they will be characterized by an energy distribution. However, we have performed calculations for different ion incident energies (between 280 and 380 eV), and the results showed that, although the different ion incident energies had a small effect on the surface recession rate, they did not influence the mechanism of reactive ion implantation and the development of aluminium oxidation. So, in first instance, this assumption of using fixed ion incident energies seems to be justified. Finally, the maximum concentration of argon inside the target is assumed to be zero because of the lack of experimental data for the depth profile of argon implantation. It should be noted that, according to previous experience with dynamic Monte Carlo codes, such a choice is reasonable when the saturation concentration of nonreactive gas in the target is not known from experiment.

In the present simulation, particular attention is paid to the choice of surface binding energies (SBE), to describe preferential sputtering effects in oxides [21]. It should be noted that preferential sputtering in the presence of oxygen has not been studied in detail. The effective surface binding energy of Ar is set to be zero. The effective surface binding energy of O and Al will be chosen in dependence on the actual surface composition by use of a matrix method. The matrix elements of surface binding energy are SBV_{O-O} , SBV_{O-Al} , SBV_{Al-O} and SBV_{Al-Al} , where $SBV_{O-Al} = SBV_{Al-O}$. These elements are evaluated by the formula [11]

$$SBV_{O-O} = 0,$$

$$SBV_{Al-Al} = \Delta H_{Al}^s,$$

$$SBV_{O-Al} = \frac{1}{2} \Delta H_{Al}^s + \frac{n+m}{2nm} \Delta H^f + \frac{n+m}{4n} \Delta H^{diss},$$

where n and m are equal to 2 and 3, respectively, because Al_2O_3 is considered here, ΔH_{Al}^s denotes the sublimation enthalpy of Al and equals 3.36 eV, ΔH^f denotes the formation enthalpy per molecule of the compound Al_2O_3 and equals 17.4 eV, and ΔH^{diss} denotes the dissociation energy of the oxygen molecule and equals 5.16 eV. SBV_{O-O} is taken zero because we neglect any interaction of O in the surface. If the concentrations of O and Al at the surface are respectively C_O and C_{Al} , we can obtain the effective SBEs of Al and O in the following way:

$$SBE(Al) = C_O \times SBV_{O-Al} + C_{Al} \times SBV_{Al-Al},$$

$$SBE(O) = C_{Al} \times SBV_{O-Al} + C_O \times SBV_{O-O}.$$

For example, at the beginning of sputtering, the target consists of pure aluminium, i.e. $C_{Al} = 1$, then $SBE(O) = 12.212$ eV and $SBE(Al) = 3.36$ eV. In this case, aluminium is preferentially sputtered. $SBE(Al)$ and $SBE(O)$ will become 8.67 and 4.88 eV, respectively, when the target surface becomes stoichiometric alumina oxide, in this case, oxygen is more easily sputtered than aluminium.

Because the incident energy of O_2^+ is very large compared to the dissociation energy of the oxygen molecule, surface collision will cause an immediate dissociation of O_2^+ . Therefore TRIDYN actually uses 180 eV as the incident energy of O^+ ions but its fluence is doubled. However, when the fluence is referred to hereafter in this paper it always means the real fluence of Ar^+ and O_2^+ ions. According to the model of DG, the implanted oxygen atoms can react with the target atoms or they can form oxygen molecules. The oxygen molecules can further react with the aluminium target or outdiffuse before reaction. In this simulation we assume no formation of oxygen molecules and the extra oxygen over the stoichiometry will outdiffuse from the target. The bulk binding energy of each target component and the cut-off energies of projectiles and target components are simply set to zero according to previous experiences with the TRIDYN simulation.

The target is divided into 200 slabs, each with initial thickness of 0.3 nm. The beam of Ar^+ and O_2^+ ions is assumed to be normal to the target surface. A proper fluence increment of 10^{12} ions/cm²

per pseudoprojectile is used, which is a good choice to reduce computer time and maintain the precision. According to DG's experiment, a fluence of 6×10^{16} ions/cm² corresponds to a sputtering time of 1 s. Thus to study the ion implantation mechanism and its steady-state behaviour, a sputter time as long as 100 s (i.e. a total fluence of 6×10^{18} ions/cm²) is used in our TRI-DYN simulation. A typical number of pseudo-projectiles varies from 10^5 to 2×10^6 depending on the applied total fluence. For convenience of description, let x denote the ratio of the pseudoparticle number of O₂⁺ ions to the sum of Ar⁺ and O₂⁺ ions. The number x is identical to the oxygen mole fraction according to the second assumption mentioned above.

3. Results and discussion

The model is used to simulate the bombardment of aluminium by Ar⁺ and O₂⁺ ions with an energy of 360 eV, at different oxygen mole fractions x .

3.1. Study of the oxidation mechanism of the target

3.1.1. Low oxygen mole fraction

Fig. 1 shows the elemental concentration ratio O/Al in the first slab (representing the surface O/Al concentration ratio) and the surface recession as a

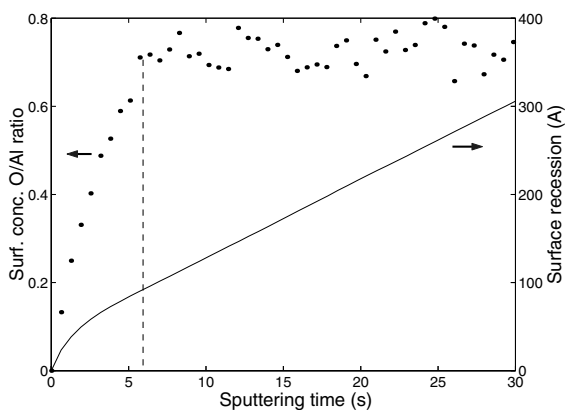


Fig. 1. Calculated elemental concentration ratio O/Al at the surface (dots, left axis) and surface recession (solid line, right axis) versus sputtering time for Ar⁺ and O₂⁺ bombardment at $x = 0.05$.

function of sputtering time at $x = 0.05$. The O/Al ratio at the surface versus the sputter time has two stages. In the first stage where the sputtering time is less than 6 s, the O/Al ratio clearly increases with the sputtering time; whereas in the second stage, i.e. after 6 s, where the total fluence is larger than 40×10^{16} ions/cm², the surface O/Al concentration ratio reaches more or less a steady state. Its maximum value in the second stage, however, never surpasses 0.8, even at very long sputtering time. The mean value is 0.706 and the standard deviation is 0.034. This observation that the maximum O/Al ratio is much less than 1.5 (i.e. the stoichiometric value for Al₂O₃) means that the target surface will never become fully oxidized at low oxygen mole fraction such as $x = 0.05$, no matter how long the sputtering time.

It appears also from Fig. 1 that the surface recession as a function of sputtering time has two stages. A positive surface recession means that the surface is eroded because of the sputtering. In the first stage the surface recession speed decreases gradually up to 6 s, which means that the target surface gradually contains more Al₂O₃ compound which has a stronger binding energy. In the second stage when the sputtering time is larger than 6 s, the surface recession increases linearly with the sputtering time, i.e. the erosion rate is constant, because the surface condition does not change anymore.

Fig. 2 presents the calculated O/Al ratio depth distribution at different sputter times. Because the position of the target surface always shifts during the sputtering, we set for convenience of comparison the surface position at the beginning of sputtering as zero in the x -axis. The shifted surface positions are indicated by the starting point of the curves at different times. For example, curve 1 in Fig. 2 shows the O/Al ratio depth profile at a sputtering time of 200 ms. At this time, the target is eroded by about 10 Å in thickness as a result of sputtering. All curves in Fig. 2 show that the penetration of implanted ions into the target is about 40 Å. Fig. 2 shows how the O/Al ratio gradually becomes larger at the target surface with increasing sputter time, because reactive ions are implanted into the target bulk. Subsurface reaction between oxygen and aluminium will occur if the reaction rate is larger than the sputter rate. As the reaction

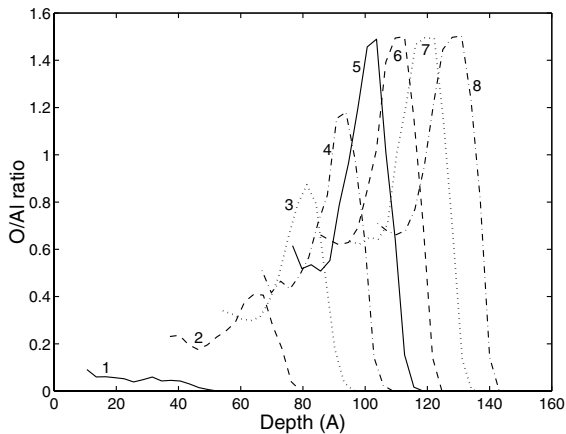


Fig. 2. Calculated O/Al ratio depth distribution for the case of $x = 0.05$ at different sputtering times: 200 ms (curve 1), 1190 ms (curve 2), 2180 ms (curve 3), 3170 ms (curve 4), 4160 ms (curve 5), 5150 ms (curve 6), 6140 ms (curve 7) and 7130 ms (curve 8).

rate depends on the reactive gas concentration in the target, a higher reactive ion fluence, which accompanies a larger sputtering time, will result in more subsurface compound formation. With increasing sputtering time, it is possible to form Al_2O_3 in the subsurface, as is shown in Fig. 2. After the compound is formed with longer sputtering time the very thin layer of alumina will “grow” towards the target surface. It should be noted that actually the target surface recedes towards the formed oxide layer due to the sputtering. Besides, in the beginning of sputtering, when the target itself only consists of aluminium, the preferential sputtering of Al, owing to the lower effective SBE of Al, also makes some contribution to the build-up of compound formation. Moreover, for the low oxygen mole fraction, the target surface cannot become fully oxidized because there are not enough oxygen ions implanted into the bulk to react with aluminium atoms. Fig. 2 shows that, with increasing sputtering time, a steady state in the O/Al ratio depth distribution is reached, as is clear from curves 6, 7 and 8 but the thin surface layer cannot evolve into full oxidation.

3.1.2. Higher oxygen mole fraction

Fig. 3 presents the calculated O/Al ratio at the surface versus sputtering time for different oxygen

mole fractions. One can clearly see that for higher oxygen mole fractions the steady state is more quickly reached and the O/Al ratio at the surface is higher. When $x = 0.2$, more or less complete oxidation at the surface is observed.

Fig. 4 shows the O/Al ratio depth profile at different sputtering times for an oxygen mole fraction $x = 0.2$. By comparing Figs. 2 and 4 one can see that the basic properties exhibited during the sputtering are the same: the possible formation of Al_2O_3 always first takes place in the target bulk and then the thin alumina layer extends towards the target surface, regardless of the oxygen mole fraction. However, it is illustrated in Fig. 4 for the high mole fraction $x = 0.2$, that the thin alumina layer continues extending towards the target surface and soon the surface becomes more or less oxidized. One may also notice that the surface recession in Fig. 4 is much slower than in Fig. 2. With increasing sputtering time, more reactive ions are implanted into the target and they react with target atoms to form chemical bonds. The latter can reduce the target erosion rate because the chemical bonds of the formed compound are generally stronger than the original target lattice bonds. It is found that oxygen mole fractions higher than $x = 0.2$ will lead to similar results as shown in Fig. 4. Furthermore, it can be deduced

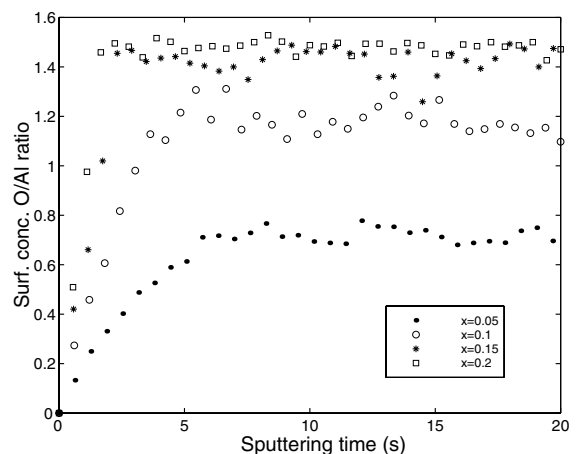


Fig. 3. Calculated O/Al ratio at the surface as a function of sputtering time for different oxygen mole fractions x : 0.05 (dots), 0.1 (circles), 0.15 (*) and 0.2 (square).

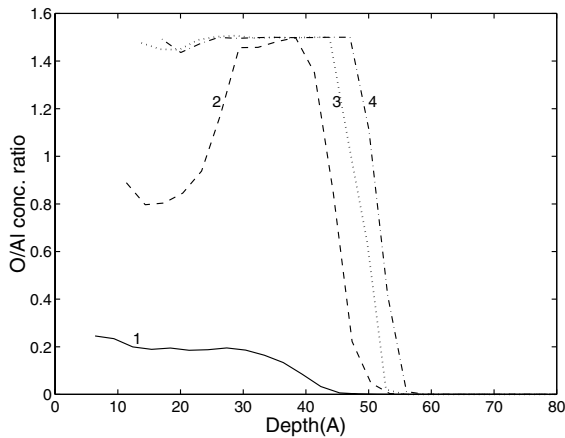


Fig. 4. Calculated O/Al ratio depth distribution for the case of $x = 0.2$ at different sputter times: 170 ms (curve 1), 1020 ms (curve 2), 1870 ms (curve 3) and 2720 ms (curve 4).

from Fig. 4 that the thickness of the thin alumina layer is about 30 Å.

The surface concentration O/Al ratio when steady state is reached (cf. Fig. 3) versus oxygen mole fraction is illustrated in Fig. 5. To be sure that steady state is reached and that the O and Al concentrations will not change anymore, the calculations were performed for a fluence of 200×10^{16} ions/cm² which corresponds to a sputter time of 33.3 s. Moreover, because the surface concentration ratio O/Al always shows some fluctuation, even when steady state is reached, we have averaged the surface concentration ratio O/Al over the period of steady state. The standard deviations are also calculated. In all calculations, the standard deviation is less than 0.05. When x is about 0.14, the averaged value of O/Al is about 1.4, and the standard deviation is 0.049. The larger standard deviation reflects the fact that the steady state is not highly stable. When x is about 0.20, the averaged value of O/Al is 1.455 but the standard deviation reduces to 0.023. It means that the target surface becomes fully oxidized when $x = 0.2$ or more.

Fig. 6 shows the calculated surface recession versus sputtering time for various oxygen mole fractions. As mentioned above, a higher oxygen mole fraction x leads to a lower surface recession rate (erosion rate), as is clear from Fig. 6(a). From

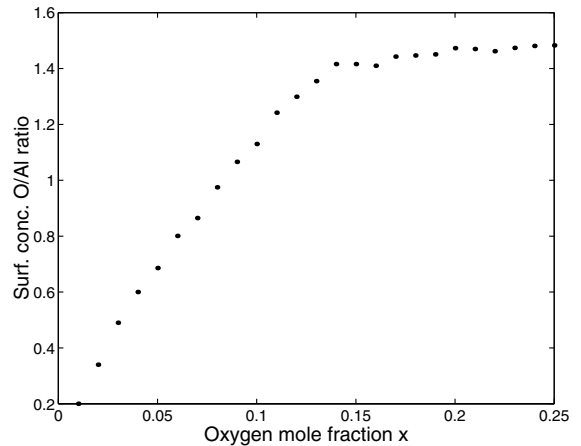


Fig. 5. Elemental concentration ratio O/Al in the first slab averaged in a steady-state period versus oxygen mole fraction x .

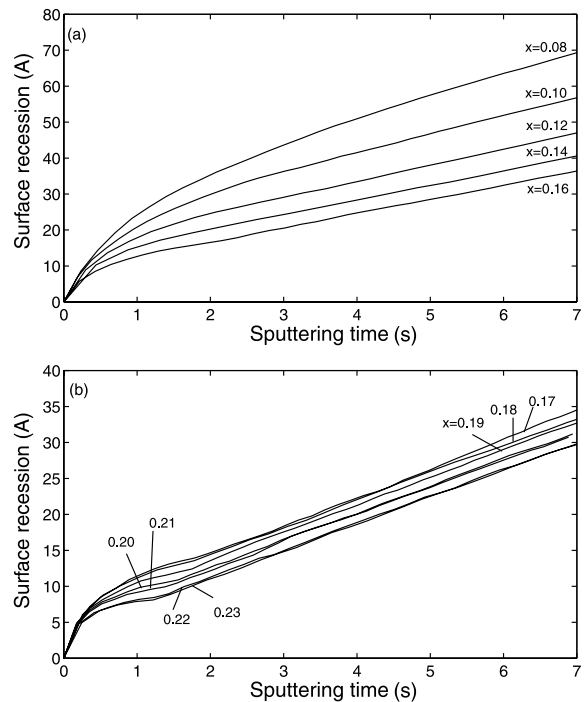


Fig. 6. Calculated surface recession versus sputtering time at different oxygen mole fractions x .

Fig. 6(a) one also can see that the two lines denoting $x = 0.14$ and $x = 0.16$ respectively become almost parallel when they enter into their own steady states. This means that in the steady state

the erosion rate almost becomes a constant when $x = 0.14$. When x increases further, the surface recession rate does not change so much any more as can be seen in Fig. 6(b). Especially when x increases up to 0.2 or even more, the surface recession rates for different x become the same. The results for x above 0.23 are not presented here because they are almost the same as that for 0.23. When an oxygen mole fraction higher than 0.2 is applied, the thin layer of compound is formed soon after the sputtering begins. It should be mentioned that, if the effective SBE of O becomes less than that of Al, the preferential sputtering of O takes place again; and the outdiffusion together with such a preferential sputtering can balance with the extra oxygen from the ion beam such that the composition of target surface does not change anymore.

3.2. Critical mole fraction for avalanche

In the above study, we have investigated the oxidation mechanism of the target, and observed a clear difference between low oxygen mole fraction ($x < 0.14$), where the target surface never becomes fully oxidized, and high oxygen mole fraction ($x > 0.14$ –0.2), where the target surface becomes fully oxidized after some time of sputtering. However, no abrupt change, or “avalanche”, in surface recession rate, as was shown in DG’s experiment, is observed in the calculations when the oxygen mole fraction x varies from 0.08 to 0.23. This suggests that, in our calculations the critical mole fraction of the avalanche phenomenon is not related to the fact whether the target surface becomes fully oxidized or not.

To investigate the avalanche phenomenon in more detail, we have performed the TRIDYN calculations at lower oxygen mole fractions. Fig. 7 presents the calculated surface recession as a function of sputtering time at very low oxygen mole fractions. The result for the case of $x = 0.05$ was already shown in Fig. 1. For the pure argon impinging on the target, the surface recession rate (erosion rate) is constant. When the target is bombarded with Ar^+ and O_2^+ ions together, the target surface condition is changed due to the reactive ion implantation into the target and chem-

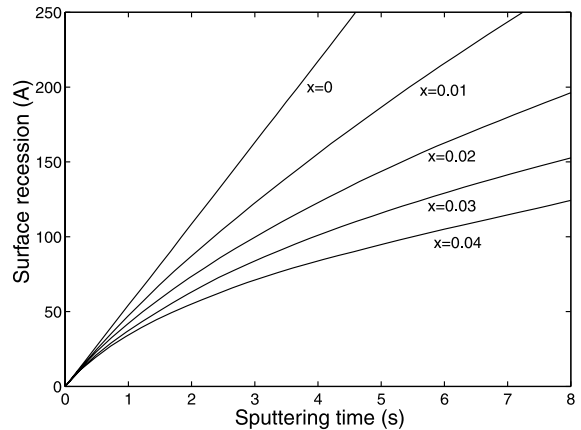


Fig. 7. Calculated surface recession versus sputtering time at different oxygen mole fractions x .

ical reaction at the subsurface. As is described in Fig. 1, the surface recession as a function of sputtering time normally can be divided into two stages. When the surface recession enters into the second stage, it reaches a steady state in which its rate does not change anymore. It is clearly seen that with increasing x , the surface recession rates become lower and lower.

To explore the critical oxygen mole fraction for the avalanche, we have done many detailed calculations for the erosion rate at various x . The erosion rate is obtained after the surface recession reaches its steady state. Fig. 8 presents the calculated erosion rate as a function of oxygen mole fraction under the conditions specified above (i.e. the incident energy is 360 eV and the total sputtering time is 100 s). One can see from Fig. 8 that the erosion rate decreases significantly from 54 Å/s at $x = 0$ to about 15 Å/s at $x = 0.0298$, but no jump in the calculated erosion rate is observed. When increasing x by a very small step, we found an abrupt change around $x = 0.03$ which is denoted by the arrow. Comparing to DG’s experiment, we can also say that this abrupt change in erosion rate indicates a transition during reactive magnetron sputtering which is not induced by an abrupt change in the reactive gas partial pressure, as generally accepted. Hence, this jump directly supports the avalanche mechanism proposed by DG although the calculated value for the critical

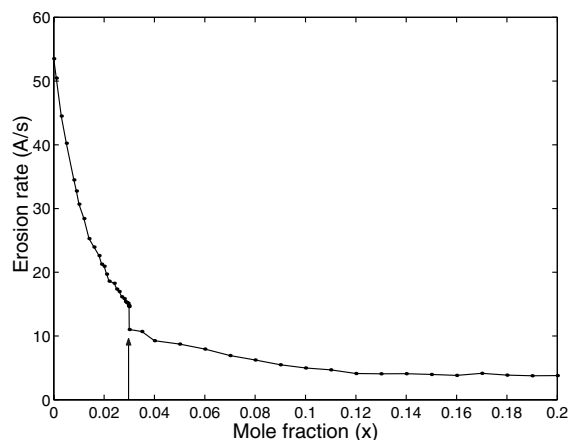


Fig. 8. Calculated erosion rate versus as a function of oxygen mole fractions x .

mole fraction ($x = 0.03$) is much lower than the experimental value ($x = 0.23$) [4]. This difference may be due to the fact that we did not take into account the chemical reaction between the reactive gas and the deposited target material on the substrate and chamber walls of the vacuum chamber. This so-called gettering process reduces the effective partial pressure in the vacuum chamber and results in a much smaller reactive gas mole fraction than expected from the ratio between the reactive gas flow and the total gas flow. Therefore, the calculated critical mole fraction for the abrupt change in erosion rate might be extended to a much higher value as compared to the calculated value. In our future work, we will try to improve our model, to obtain a calculated critical mole fraction in better agreement with experiment. However, it should be realized that a theoretical prediction of this avalanche phenomenon has never been reported before.

4. Summary

In the experiment reported by [4], the voltage of an aluminium target was found to change during magnetron sputtering when oxygen is added to the argon plasma. From this experiment, it was pointed out that chemisorption alone cannot be responsible for the voltage change or target surface

modification. A reactive ion implantation mechanism and chemical reaction occurring under the surface were thus proposed. To check this idea and to understand the mechanism in detail, a dynamic Monte Carlo modelling was performed in the present work. The simulation code TRIDYN was applied to simulate the bombardment of Ar^+ and O_2^+ ions on an aluminium target, to investigate the reactive sputtering of aluminium in a magnetron discharge. By calculating the surface concentration ratio O/Al and the surface recession as a function of sputtering time, as well as the O/Al ratio depth profiles, we have found that for all oxygen mole fractions, the formation of aluminium oxide always takes place first at the subsurface instead of in the surface. At oxygen mole fraction below 0.14, the target surface can never become fully oxidized, even at very long sputtering times. When the oxygen mole fraction reaches 0.14–0.2, the target surface becomes more or less fully oxidized.

Moreover, we have investigated the calculated surface recession rate (erosion rate) as a function of oxygen mole fraction and found an abrupt change in the erosion rate for $x = 0.03$. This change reflects the occurrence of avalanche and the mode transition from metallic to poisoned sputtering although the theoretically predicted critical mole fraction is much lower than the experimentally observed value. There are several reasons for this difference, but the most important one is that the gettering of substrate on the wall in the vacuum chamber has not been included into our model. However, our numerical results qualitatively confirm the reactive ion implantation mechanism and the chemical reaction occurring at the subsurface as well as the avalanche phenomenon proposed in [4].

Acknowledgements

Z.Y. Chen is financed by the Bilateral scientific and technological cooperation (Joint Project No. BIL 99/46) of the Ministry of the Flemish Community, the Ministry of Science and Technology of China, and the National Science Foundation of China. A.B. is indebted to the Flemish Fund for Scientific Research (FWO) for financial support.

The authors also acknowledge financial support from the Belgian Federal Services for Scientific, Technical, and Cultural Affairs (DWTC/SSTC) of the Prime Minister's Office through IUAP-V. We are grateful to R. Gijbels and R. De Gryse for their fruitful discussions. Finally, we would like to thank W. Möller for supplying the simulation code TRIDYN (Version 4.0).

References

- [1] B. Chapman, *Glow Discharge Processes*, Wiley, New York, 1988.
- [2] R.K. Waits, *Thin Film Processes*, Academic, Orlando, FL, 1978.
- [3] S. Maniv, W.D. Westwood, *Surf. Sci.* 100 (1980) 108.
- [4] D. Depla, R. De Gryse, *Plasma Sources Sci. Technol.* 10 (2001) 547.
- [5] W.G. Johanson, W.G. Carruthers, *J. Vac. Sci. Technol. A* 5 (1987) 2246.
- [6] A. Ershov, L. Pekker, *Thin Solid Films* 289 (1996) 140.
- [7] L.B. Jonsson, T. Nyberg, S. Berg, *J. Vac. Sci. Technol. A* 17 (1999) 1827.
- [8] S. Berg, H.-O. Blom, T. Larsson, C. Nender, *J. Vac. Sci. Technol. A* 5 (1987) 502.
- [9] E. Kusano, *J. Appl. Phys.* 87 (2000) 2015.
- [10] D. Depla, A. Colpaert, K. Eufinger, A. Segers, J. Haemers, R. De Gryse, *Vacuum* 66 (2002) 9.
- [11] W. Möller, W. Eckstein, J.P. Biersack, *Comput. Phys. Commun.* 51 (1988) 355;
W. Möller, M. Posselt, *TRIDYN_FZR User Manual*.
- [12] W. Eckstein, *Computer Simulation of Ion–Solid Interaction*, Springer, Berlin, 1991.
- [13] J.P. Biersack, W. Eckstein, *Appl. Phys. A* 34 (1984) 73.
- [14] S.S. Todorov, I.R. Chakarov, V. Miteva, D.S. Karpuzov, D.V. Klyachko, V.V. Uvarov, V. Shinkorenko, *Surf. Sci.* 271 (1992) 641.
- [15] J.W. Bradley, G. Lister, *Plasma Sources Sci. Technol.* 6 (1997) 524.
- [16] N.F. Cramer, *J. Phys. D: Appl. Phys.* 30 (1997) 2573.
- [17] T.E. Sheridan, M.J. Goeckner, J. Goree, *J. Vac. Sci. Technol. A* 8 (1990) 30.
- [18] S. Ido, M. Kashiwagi, M. Takahashi, *Jpn. J. Appl. Phys.* 38 (1999) 4450.
- [19] K. Nanbu, S. Segawa, S. Kondo, *Vacuum* 47 (1996) 1013.
- [20] K. Nanbu, K. Mitsui, S. Kondo, *J. Phys. D: Appl. Phys.* 36 (2000) 4808.
- [21] R. Kelly R, *Nucl. Instr. and Meth. B* 18 (1987) 388.